Nuclear Inst. and Methods in Physics Research, A 910 (2018) 90–95

Contents lists available at ScienceDirect

Nuclear Inst. and Methods in Physics Research, A

journal homepage: www.elsevier.com/locate/nima

Monte-Carlo based performance assessment of ASACUSA's antihydrogen detector

Y. Nagata [a,b,*], N. Kuroda [c], B. Kolbinger [d], M. Fleck [d,1], C. Malbrunot [d,e], V. Mäckel [d,2], C. Sauerzopf [d,3], M.C. Simon [d], M. Tajima [c,4], J. Zmeskal [d], H. Breuker [e], H. Higaki [f], Y. Kanai [g], Y. Matsuda [c], S. Ulmer [b], L. Venturelli [h,i], E. Widmann [d], Y. Yamazaki [b]

[a] Department of Physics, Tokyo University of Science, 1-3 Kagurazaka, Shinjuku, 162-8601 Tokyo, Japan
[b] Ulmer Fundamental Symmetries Laboratory, RIKEN, 2-1 Hirosawa, Wako-shi, 351-0198 Saitama, Japan
[c] Institute of Physics, University of Tokyo, 3-8-1 Komaba, Meguro-ku, 153-8902 Tokyo, Japan
[d] Stefan-Meyer-Institut für Subatomare Physik, Österreichische Akademie der Wissenschaften, Wien 1090, Austria
[e] CERN, Genève 1211, Switzerland
[f] Graduate School of Advanced Sciences of Matter, Hiroshima University, 739-8530 Hiroshima, Japan
[g] RIKEN Nishina Center for Accelerator-Based Science, 2-1 Hirosawa, Wako-shi, 351-0198 Saitama, Japan
[h] Dipartimento di Ingegneria dell'Informazione, Università di Brescia, Brescia 25133, Italy
[i] Istituto Nazionale di Fisica Nucleare, Sez. di Pavia, I-27100 Pavia, Italy

ARTICLE INFO

Keywords:
Antihydrogen
Antimatter
Detector
Calorimeter
Tracker

ABSTRACT

An antihydrogen detector consisting of a thin BGO disk and a surrounding plastic scintillator hodoscope has been developed. We have characterized the two-dimensional positions sensitivity of the thin BGO disk and energy deposition into the BGO was calibrated using cosmic rays by comparing experimental data with Monte-Carlo simulations. The particle tracks were defined by connecting BGO hit positions and hits on the surrounding hodoscope scintillator bars. The event rate was investigated as a function of the angles between the tracks and the energy deposition in the BGO for simulated antiproton events, and for measured and simulated cosmic ray events. Identification of the antihydrogen Monte Carlo events was performed using the energy deposited in the BGO and the particle tracks. The cosmic ray background was limited to 12 mHz with a detection efficiency of 81%. The signal-to-noise ratio was improved from 0.22 $s^{-1/2}$ obtained with the detector in 2012 to 0.26 $s^{-1/2}$ in this work.

1. Introduction

Recently, antihydrogen ($\bar{H}$) atoms have been produced [1] in a unique cusp trap [2–4] developed for the in-flight hyperfine spectroscopy of ground state $\bar{H}$ atoms [5–7]. The most recent progress is reported in [8–10]. In 2012, the ASACUSA Cusp collaboration developed a $\bar{H}$ detector consisting of a BGO ($Bi_4Ge_3O_{12}$) scintillator disk in combination with a single anode photomultiplier (PMT) and 5 plastic scintillator plates. The detector was able to reject cosmic backgrounds with a high efficiency [11]. In order to further improve the background rejection efficiency, we have developed a new $\bar{H}$ detector. The single anode PMT has been replaced by 4 multi-anode PMTs (MAPMTs) for 2D photon readout of the BGO. The five plastic scintillators were replaced by a two-layer hodoscope with 32 plastic scintillator bars per layer to determine charged particle tracks with higher resolution [12].

2. $\bar{H}$ detector

Fig. 1 shows a schematic diagram of the structure of the new $\bar{H}$ detector consisting of the thin BGO disk and the hodoscope. The BGO disk, has a diameter of 90 mm and a thickness of 5 mm and is housed on the vacuum side (10^{-7} Pa) of a UHV viewport. The front surface of the BGO disk was coated with a carbon layer of thickness 0.7 μm to reduce multireflections of the light from scintillation on the surface. It was found that the carbon coating improved the position resolution by a factor of ~2 in our previous device [13]. To achieve a position sensitive readout, 4 MAPMTs (Hamamatsu H8500C) each having 8 × 8 anodes with effective area of 49 mm × 49 mm were directly placed on the view port glass as shown in Fig. 2. The output of 8 × 8 anodes were amplified, digitized and stored by an amplifier unit (Clear Pulse 80190) which was

* Corresponding author at: Department of Physics, Tokyo University of Science, 1-3 Kagurazaka, Shinjuku, 162-8601 Tokyo, Japan.
E-mail address: yugo.nagata@rs.tus.ac.jp (Y. Nagata).
[1] Present address: Institute of Physics, University of Tokyo, 3-8-1 Komaba, Meguro-ku, 153-8902, Tokyo, Japan.
[2] Present address: Ulmer Fundamental Symmetries Laboratory, RIKEN, 2-1 Hirosawa, Wako-shi, 351-0198, Saitama, Japan.
[3] Present address: Data Technology, Vienna, Austria.
[4] Present address: RIKEN Nishina Center for Accelerator-Based Science, 2-1 Hirosawa, Wako-shi, 351-0198, Saitama, Japan.

https://doi.org/10.1016/j.nima.2018.09.013
Received 11 June 2018; Received in revised form 4 September 2018; Accepted 4 September 2018
Available online xxxx

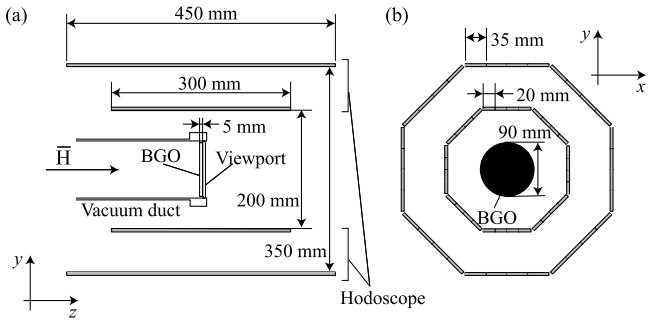

Fig. 1. Cross section of the H̄ detector along the beam axis (a) and perpendicular to the H̄ beam axis (b).

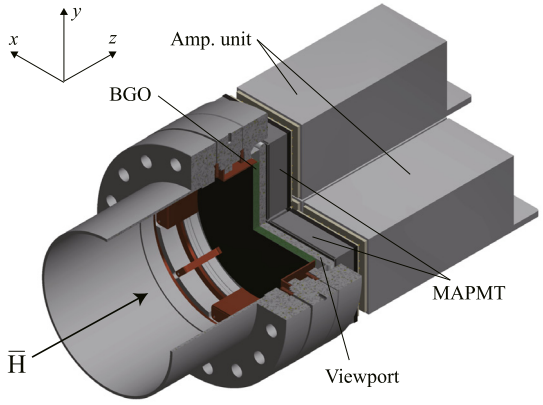

Fig. 2. Three quarter section view of the 2D sensitive BGO detector.

a dedicated model for the H8500C and included 8 × 8 charge amplifiers and analogue-to-digital converters with 12 bit resolution.

The hodoscope consists of two layers of 32 plastic scintillator bars arranged in an octagonal configuration [12]. The scintillator bars are 300 mm × 20 mm × 5 mm for the inner layer and 450 mm × 35 mm × 5 mm for the outer. With face to face distances of 200 mm and 350 mm respectively for the inner and outer layers (see Fig. 1(a)). The solid angle covered by the scintillator bars in units of 4π seen from the center of the BGO is $\omega \sim 80\%$. Silicon photomultipliers (SiPM, KETEK PM3350TS) were connected to both ends of each bar. The output pulses from the SiPMs was amplified by dedicated front end modules described in detail elsewhere (see Ref. [14]) and recorded by 128 channels waveform digitizers (CAEN V1742).

Meshes to which a high voltage can be applied is installed at the upstream of the detector to reject the antiprotons leaking from the cusp trap for the measurement of the H̄ atoms [15].

3. 2D distribution of cosmic rays

To obtain the relative sensitivity of each channel, 4 MAPMTs were assembled and irradiated by pulsed (200 ns width) light from a LED with the peak wavelength of 470 nm (see also Ref. [13]), the peak emission wavelength of the BGO scintillation light was 480 nm. The voltages applied to the MAPMTs were adjusted such that the total output charge of each MAPMT were equal.

Fig. 3(a) shows an example of a 2D map of output charges from one of the 4 MAPMTs averaged over 10^4 pulses of LED light. The channel with the maximum output charge is arbitrarily set to 100 and all other channels are scaled accordingly. The relative gain of the channels of each MAPMT are evaluated using this mapping. This result was compared with the data sheet from the manufacturer where a tungsten filament lamp was used for calibration. By taking the ratio between

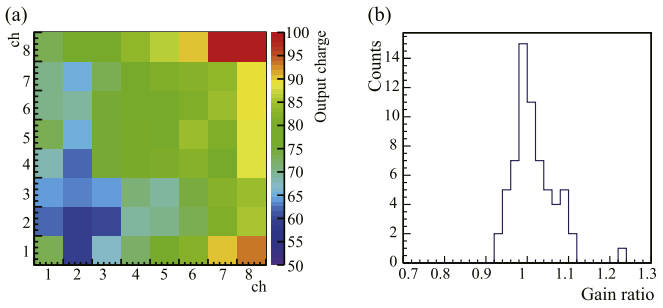

Fig. 3. (a) Example of a 2D map of averaged output charges of one of the 4 MAPMTs investigated by LED light. (b) Distribution of the gain ratio between the measured values and the data sheet values for each channel.

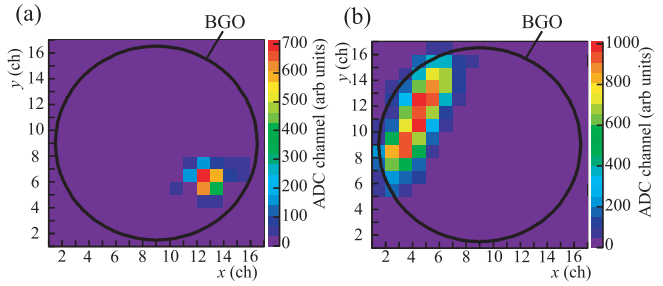

Fig. 4. Examples of 2D charge distributions of cosmic rays events where the BGO surface has been penetrated nearly perpendicularly (a) or at grazing incidence (b).

the measured values and those from the data sheet for each anode, the distribution of the gain ratio as shown in Fig. 3(b) was obtained. The standard deviation of this distribution is around 5%.

Fig. 4(a) and (b) show the 2D charge distribution for two example cosmic rays events after offline gain matching of the individual MAPMT channels described above. In these examples, the BGO surface has been penetrated nearly perpendicularly (a) or at grazing incidence (b). These figures demonstrate that position sensitive readout has been successfully implemented using 2D MAPMTs.

In order to reconstruct particle tracks (to be discussed in detail later), we define the position of a hit on the BGO as the center of the anode giving the highest output charge. When the hit positions observed in the 2D distribution are outside of the BGO, such events are removed in the analysis because they are probably Čerenkov light generated in the optics of the MAPMT or the viewport when high energy charged particles pass through them. The total charge Q is obtained by summing the charges from all channels (see Fig. 4(a) and (b)).

4. Energy calibration of the BGO detector

For the energy calibration, cosmic rays were measured and the charge distribution $f(Q)$ was compared with the energy deposition distribution $g(E)$ calculated by a Monte-Carlo simulation using the Geant4 toolkit[5] [16]. Blue solid circles in Fig. 5 show $f(Q)$ for cosmic rays events when more than 2 inner hodoscope bars are hit in any coincident combination. A bar is considered to be 'hit' when there is a coincidence between the signals of the upstream and downstream SiPMs connected to the bar.

The simulation includes the BGO detector together with the viewport and the vacuum duct (see Fig. 1(a)). Cosmic rays are generated by the CRY package [17]; Čerenkov light however is not included. $g(E)$

[5] Geant4.9.6 Patch-02 was used.